ACS APPLIED MATERIALS
& INTERFACES

Research Article

Enhanced Electrospinning of Active Organic Fibers by Plasma Treatment on Conjugated Polymer Solutions

Vito Fasano,[+] Romolo Laurita,[+] Maria Moffa, Chiara Gualandi, Vittorio Colombo, Matteo Gherardi, Eyal Zussman, Gleb Vasilyev, Luana Persano, Andrea Camposeo, Maria Letizia Focarete,* and Dario Pisignano*

Read Online

ACCESS | 📊 Metrics & More | 📄 Article Recommendations | ⓢ Supporting Information

ABSTRACT: Realizing active, light-emitting fibers made of conjugated polymers by the electrospinning method is generally challenging. Electrospinning of plasma-treated conjugated polymer solutions is here developed for the production of light-emitting microfibers and nanofibers. Active fibers from conjugated polymer solutions rapidly processed by a cold atmospheric argon plasma are electrospun in an effective way, and they show a smoother surface and bead-less morphology, as well as preserved optical properties in terms of absorption, emission, and photoluminescence quantum yield. In addition, the polarization of emitted light and more notably photon waveguiding along the length of individual fibers are remarkably enhanced by electrospinning plasma-treated solutions. These properties come from a synergetic combination of favorable intermolecular coupling in the solutions, increased order of macromolecules on the nanoscale, and resulting fiber morphology. Such findings make the coupling of the electrospinning method and cold atmospheric plasma processing on conjugated polymer solutions a highly promising and possibly general route to generate light-emitting and conductive micro- and nanostructures for organic photonics and electronics.

KEYWORDS: *Light-emitting nanofibers, Conjugated polymers, Electrospinning, Cold atmospheric pressure plasma, Photoluminescence, Waveguiding*
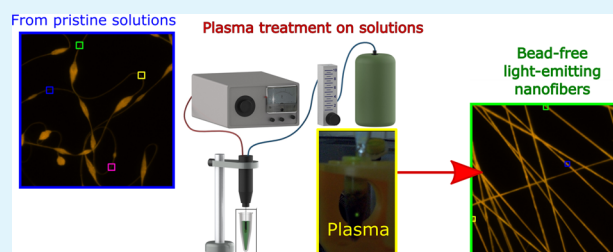
INTRODUCTION

Active organic micro- and nanofibers have raised growing interest in the last decade, with fields of applications ranging from photonics[1−4] to nanoelectronics,[5−7] wearables,[8] energy conversion, and soft robotics.[9−11] This has been motivated by the intriguing physical properties of this class of nanostructures, such as extremely large aspect ratio and specific surface area, remarkable optical anisotropy as well as photon transport along their longitudinal axis, enhanced charge transport, thermal conductivity, high flexibility, and mechanical robustness.[1,6,12−15] In addition, organic nanofibers can be realized with compositional and functional versatility and by low-cost manufacturing and processing methods.[16,17] Manufacturing techniques for the realization of polymeric, elongated micro- and nanostructures are numerous and include both bottom-up and top-down approaches,[18] such as interfacial polymerization,[19] synthesis in porous templates,[1,20] self-assembly,[21,22] solution blowing,[23] and electrospinning.[24−26]

The electrospinning process, which consists of realizing nanofibers by electrified semidilute polymer solutions, has become especially popular for a number of reasons. First, it is a relatively high-throughput technology that can be effectively up-scaled to industry. Second, individual electrospun fibers, which are highly interesting for applications in nanoelectronics,

photonics, and energy harvesting, can be collected by using motorized stages carrying the deposition substrate and rapidly crossing the trajectory of electrospun jets, as well as by various types of parallel electrodes supporting gaps through which fibers can be suspended, or other conductive frames.[4,27,28] In addition, near-field electrospinning methods can be employed to deposit individual fibers and patterns made of them in a highly controlled way.[29,30] Third, filament-shaped nanostructures can be electrospun with an intrinsic orientation of molecular backbones along the fiber axis, owing to solution jet high-stretching by the electrostatic field applied during the fabrication process.[13,31−33] This feature might, in turn, improve charge carrier mobility, polarization properties of emitted light, and fiber stiffness. In this respect, electrospinning conjugated, i.e., conductive or light-emitting, polymers through a reliable process is highly desirable since these compounds show unique

combinations of electronic, optical, and mechanical properties,[34,35] which make them fundamental building blocks of plastic electronics and photonics.[36] Designing electrospinning technologies capable of effectively processing conjugated polymers could open new application fields and perspectives for embedding electronically and optically active nanostructures within flexible, wearable, and implantable devices.

Unfortunately, notwithstanding a few successful experiments with polyphenylenevinylene, polythiophene, and polyfluorene derivatives,[5,37−40] the electrospinning of conjugated polymer fibers is still a nonstandardized and challenging process. This is due to properties inherent to the materials, such as relatively low molecular weight and level of entanglement, polymer chain rigidity, the propensity to gel at high concentration, and the low solubility. Approaches to tackle these difficulties made use of blends with inert polymers that show more favorable plastic behavior and better spinnability,[41,42] which in principle can affect the properties of pristine conjugated molecules. In another method, conjugated polymers were segregated in the inner region of core−shell electrospun nanofibers realized from compound solution jets and surrounded by an external layer made with an easily electrospinnable polymer (polyvinylpyrrolidone).[37,38,43] Also, electrospinnable precursor solutions could be employed, which can then be cured to lead to conjugated polymer nanofibers, as generally performed with poly(p-phenylenevinylene).[44,45] These methods are elegant but poorly versatile in terms of conjugated polymer species as each approach relies on highly specific interfacial or polymerization chemistry and process operation. Efforts to develop a general method for the electrospinning of conjugated polymers were mainly focused on optimizing the used solvents. Good solvents for conjugated polymers are generally weakly conductive and show low boiling points, which strongly disfavors the electrospinning process.[46,47] Instead, binary mixtures of good and poor solvents were found to improve the electrospinnability of various compounds.[39,46] On the other hand, nanostructures electrospun by using a single good solvent might exhibit a higher degree of internal molecular alignment, as well as better optical performance, including a higher polarization ratio of their light emission.[31] Indeed, conjugated compounds are highly sensitive to the composition of their local microenvironment, which can strongly affect their electronic and emission properties through chain modifications and interactions with solution additives.

An innovative and very effective approach to improve the electrospinnability of polymers consists of preliminarily treating organic solutions by atmospheric plasmas.[48,49] A cold atmospheric pressure plasma (CAP) is an ionized gas consisting of electrons, positive and negative ions, excited atoms and molecules, radicals, and photons, with the electronic temperature being much higher than the macroscopic temperature. Recent work found that plasma treatments lead to the formation of smooth and bead-free polylactic acid fibers electrospun from a dichloromethane solution, without the use of other solvents with high conductivity.[50] The efficacy of this method was tested with several nonconjugated systems, such as poly(vinylidene fluoride) (PVDF)[51] and poly(ε-caprolactone) (PCL).[52] In this work, it is demonstrated that active, uniform, continuous, and smooth conjugated polymer fibers can be obtained by electrospinning of solutions treated by a CAP under proper process conditions. No blend, core−shell structure, or solvent mixture is needed, and purely conjugated filaments are obtained that show excellent morphology and

drastic reduction of bead formation compared to fibers electrospun from untreated solutions. Furthermore, the CAP treatment leaves the pristine optical properties of conjugated polymers largely unaltered and improves significantly waveguiding of light emitted from individual fibers. These results are highly promising when designing a general route to electrospun nanostructured materials by conductive and light-emitting polymers.

RESULTS AND DISCUSSION

A dielectric barrier discharge (DBD) plasma jet is used on tetrahydrofuran (THF) solutions of the two conjugated polymers, poly[(9,9-dioctylfluorenyl-2,7-diyl)-alt-co-(1,4-benzo-{2,1′,3}-thiadiazole)] (F8BT) and poly[(9,9-dioctyl-fluorenyl-2,7-diyl)-co-(1,4-diphenylene-vinylene-2-methoxy-5-{2-ethylhexyloxy}-benzene)] (PFV, see details in Methods). The chemical structures of the two polymers are shown in Figure 1a,b, respectively, and the setup for CAP-treating
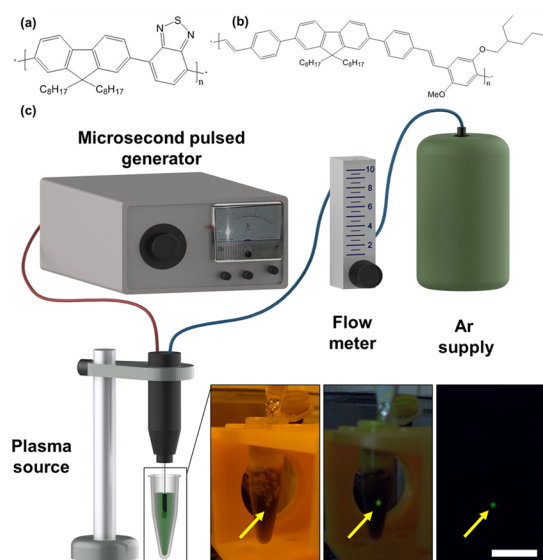
Figure 1. (a,b) Chemical structures of the light-emitting conjugated polymers, F8BT (a) and PFV (b). (c) Experimental setup for CAP treatment of conjugated polymer solutions. Bottom insets, from left to right: photograph of the conjugated polymer solution under ambient illumination and of the generated discharge (highlighted by arrows) imaged with low illumination and in the dark. Scale bar = 1 cm.

conjugated polymer solutions is schematized in Figure 1c. For the CAP treatment, the metallic needle of the plasma source is immersed in the conjugated polymer solution (1 mL), and Ar is used as working gas upon 30 kV pulsed voltage excitation at a frequency of 22 kHz for 5 min. The duration of CAP treatment on polymeric solutions must be calibrated depending on the used solution volume since very long processes are known to not lead to further improvement in the morphology of electrospun fibers[50] and might lead to a large increase of concentration in polymer solutions due to solvent evaporation. In the case of conjugated polymer solutions, these aspects might be even more critical, and any potential plasma-induced deterioration of the emissive properties of the organic materials must be avoided. A bright and localized emission can be clearly seen in our polymer solutions nearby the CAP needle upon plasma activation, as highlighted by the arrows in the bottom insets of Figure 1c.
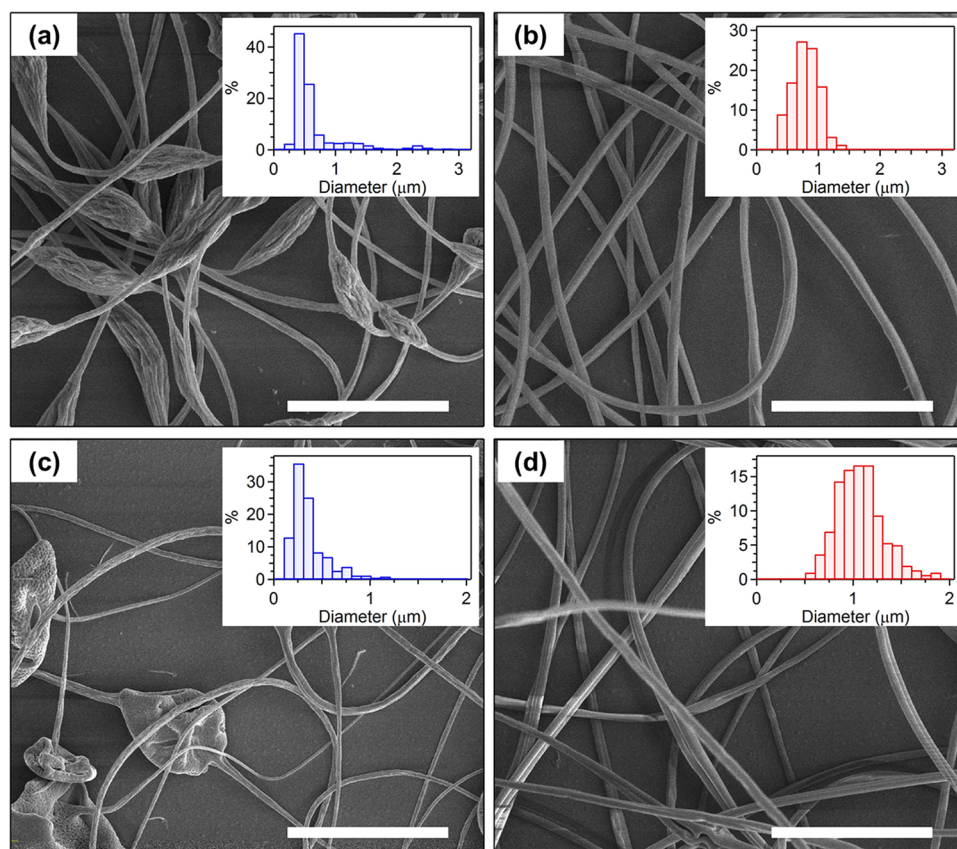
Figure 2. SEM micrographs of fibers made of F8BT (a,b) and PFV (c,d), electrospun from pristine (a,c) and CAP-treated (b,d) solutions. Scale bars: 10 (a,b), 20 μm (c,d). Insets: corresponding distributions of fiber diameters.

The morphology of F8BT and PFV fibers electrospun from either CAP-treated or pristine solutions is compared in Figure 2 and in Figures S1 and S2 in the Supporting Information. The distributions of fiber diameters are shown in the corresponding insets. Scanning electron microscopy (SEM) images highlight the eventual presence of beads, inhomogeneity, or defects along the conjugated polymer fibers. Electrospun fibers from pristine conjugated polymer solutions in THF show a somehow textured surface with shallow recessed features and significant presence of irregular beads along their length (Figure 2a,c), in agreement with previous reports.[31] Instead, fibers with a highly smooth surface are electrospun from CAP-treated solutions (Figure 2b,d). In these samples, beads are absent or very rare (Figures S1, S2).

The improvement of the morphology of fibers[48,50] electrospun from CAP-treated solutions might be due to a number of synergetic mechanisms, which include ionization of polymer chains and solvent molecules, with a consequent increase of the overall solution conductivity, as well as enhanced intermolecular interactions between ionized species, leading to changes in the viscosity and in the surface tension. While these and other aspects have been investigated in depth in aqueous solutions,[53,54] much less is known about the interaction of nonthermal plasmas with organic solvents and complex molecular systems. For instance, Grande et al.[52] found remarkable effects from plasma on PCL in chloroform and N,N-dimethylformamide and associated the observed increase of solution conductivity and viscosity with solvent molecule degradation, formation of polar species, and expansion of the polymer coils. Similar findings were reported by Colombo et

al.,[50] who studied the electrospinnability of polylactic acid in dichloromethane, and by Laurita et al.[51] for PVDF solutions in acetone/dimethyl sulfoxide mixtures, suggesting favored interactions between macromolecular chains occurring upon plasma treatment of polymeric solutions. In order to probe potential mechanisms that lead to improved electrospinnability of conjugated polymers, we first investigate the transition temperatures of here realized fibers by differential scanning calorimetry (DSC).

Figure 3a,b (c,d) shows the first heating scan and the second heating scan after quench, respectively, for PFV (F8BT) electrospun fibers. DSC curves of PFV fibers obtained from CAP-treated and pristine solutions do not show significant changes (Figure 3a,b). The only measurable thermal transition in the calorimetric curve is endothermic, around 90 °C, which is attributed to the polymer glass transition.

Instead, for F8BT fibers, several differences in thermal transitions are evidenced during the first DSC scans (Figure 3c), as better explained below. An endothermic transition is found at about 150 °C, ascribable to a transition from a glassy to a rubbery state.[55] The glass transition is followed by a crystallization exothermic peak centered at about 175 °C and by a complex melting and recrystallization transition ranging from 200 to 240 °C ascribable to polymer melting into a liquid crystalline phase. The presence of the broad endotherm featuring a double melting peak can be associated with the presence of a dispersed polymer. In F8BT fibers electrospun from pristine solutions, DSC highlights heat flows associated with crystallization and melting phenomena that are significantly less intense than those observed for fibers
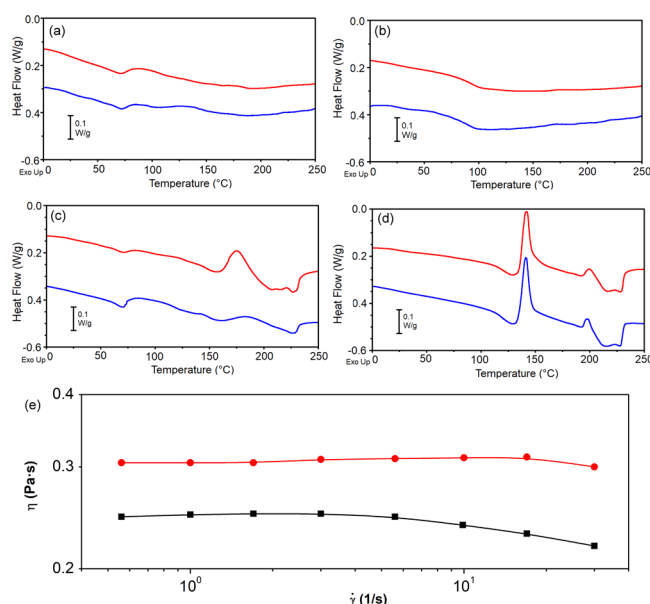
Figure 3. DSC curves of PFV (a, first heating scans, b, second heating scans after quench) and F8BT (c, first heating scans, d, second heating scans after quench) electrospun fibers. Blue curves: fibers from pristine THF solutions. Red curves: fibers from CAP-treated solutions. Flow curves of neat F8BT solution (red curve) and CAP-treated F8BT solution (black curve) (e).

electrospun from CAP-treated solutions. Such a difference in the first DSC scans can be explained by hypothesizing that, albeit the fast solvent evaporation during electrospinning generally limits the formation of ordered, regularly structured phases, the CAP could promote enhanced molecular interactions in the solution to induce such relatively less disordered F8BT domains. In fact, in the second heating scans after quench (Figure 3d), no difference can be observed between the two materials since melting erases the previous conformational history of the F8BT fibers. In the second scans, however, both the glass transition (~120 °C) and the crystallization (~140 °C) peaks are anticipated at lower temperatures, as primed by the previously reached organized phase and in agreement with literature data.[55] The rheological properties of pristine and CAP-treated F8BT solutions are also investigated and displayed in Figure 3e as flow curves, which show the dependencies of the system viscosity (η) on the applied shear rate. The behavior of the pristine solution might be considered as pseudoplastic. In fact, the viscosity is almost constant (~0.3 Pa s) at low shear rates, and then shear thinning occurs at higher rates. Following CAP treatment, a pseudoplastic behavior is retained with a slight decrease of the zero-shear rate viscosity value to 0.24 Pa s. It is noteworthy that the viscosity unexpectedly decreases by up to 10% in the whole range of rates applied, which is markedly different from previous results for nonconjugated polymers such as poly-ethylene oxide[48] and PVDF.[51] Considering the semirigid molecular structure of F8BT and its capability to assemble in liquid-crystalline structures,[55,56] the decrease of the solution viscosity found can be related to the enhancement of π-π stacking interchain interactions promoted by plasma, with the consequent formation of anisotropic solutions with lower viscosity typical for lyotropic liquid crystals.[57,58] The formation of domains with enhanced interchain interactions is further confirmed by the change of particle size and ζ-potential

measured on the F8BT solution after plasma treatment. Indeed, for the pristine solution, an average particle size of (11.5 ± 0.1) nm and a ζ-potential of −41.4 mV are measured that, following CAP treatment, change to (460.0 ± 0.3) nm and −13.4 mV, respectively. Here, the low value of particle size and the highly negative electrokinetic potential in the starting solution indicate the presence of well-dispersed and disaggregated polymer chains, whereas the concomitant increases of particle size and ζ-potential suggest the onset of polymer aggregate species promoted by plasma. Finally, different morphologies are found when casting the pristine and CAP-treated F8BT solutions onto glass (Figure 4). In the case of the
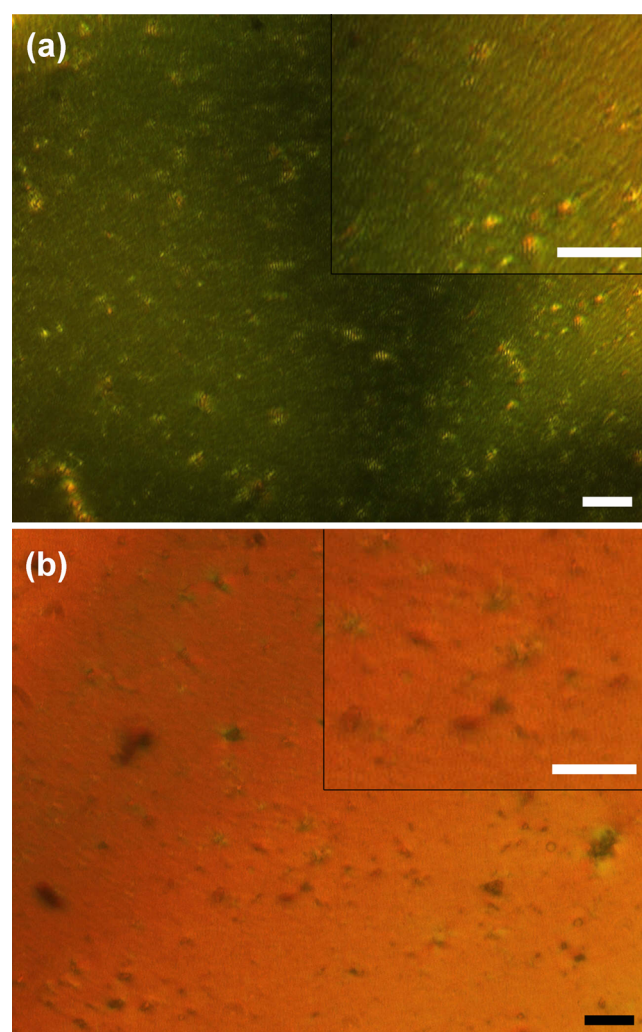
Figure 4. Optical micrographs of F8BT films cast from CAP-treated (a) and pristine (b) F8BT solutions. Images are obtained through cross polarizers. Scale bar: 20 μm. Insets: zoom at higher magnifications. Scale bar: 20 μm.

CAP-treated polymer, a nematic liquid crystal microstructure[59] can be observed through cross polarizers (Figure 4a). Different domains can be observed with microstructure alignment changing across the imaging field (inset of Figure 4a). Differently, cast samples from the pristine F8BT solution are not found to exhibit oriented textures (Figure 4b). Taken together, these results are in line with previously suggested mechanisms,[48,50,51] where the improvement of electrospinnability and reduced amount of structural defects in fibers
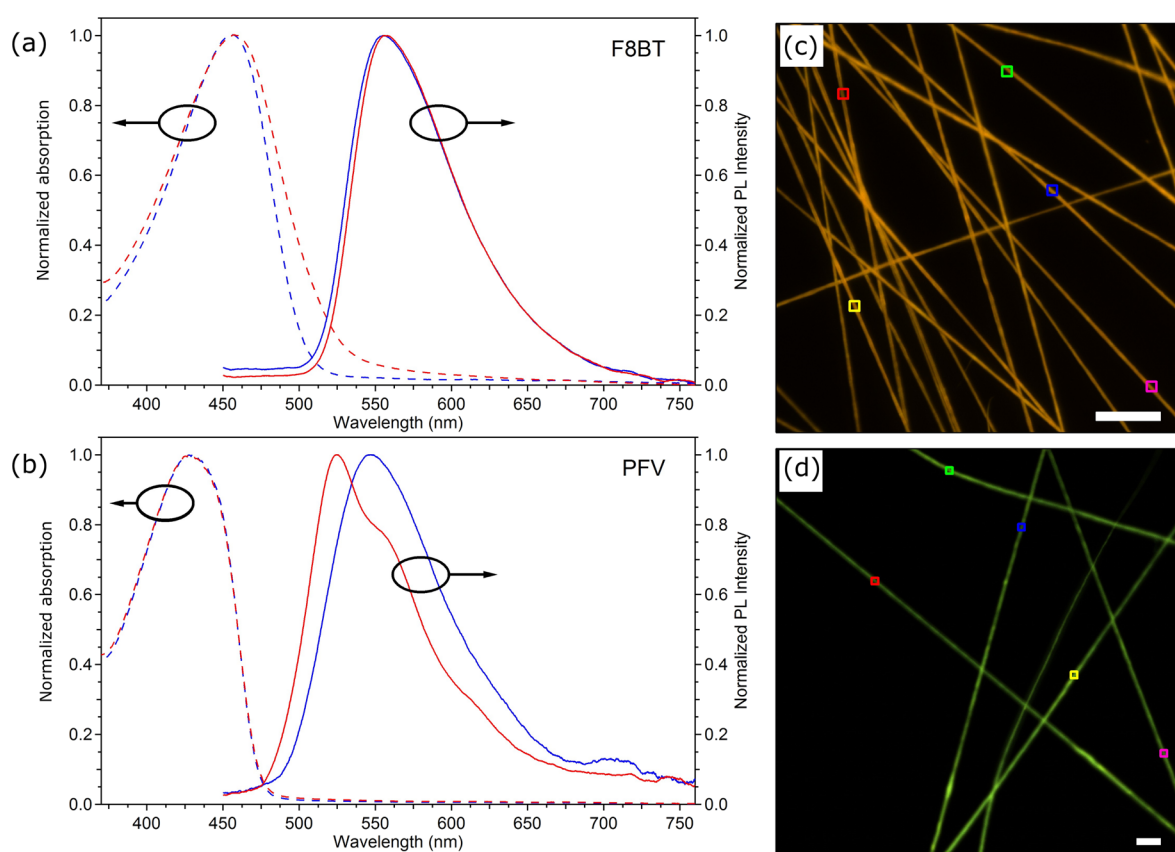
Figure 5. (a,b) Normalized absorption spectra of F8BT (a) and PFV (b) solutions (dashed lines, left vertical scales) and normalized PL spectra of F8BT (a) and PFV (b) electrospun fibers (continuous lines, right vertical scales). Blue and red lines represent pristine and CAP-treated conjugated polymer solutions, respectively. (c,d) Fluorescence confocal micrographs of light-emitting fibers electrospun from CAP-treated F8BT (c) and PFV (d) solutions. Excitation wavelength = 408 nm. Scale bar = 20 μm.

deposited upon plasma treatment of polymeric solutions might be associated with varied supramolecular interactions.

The generation of intense UV radiation, active radicals, and shock waves by plasma could be in principle detrimental to light-emitting polymers, potentially promoting a variety of damage mechanisms, which could include multiple possible defect activation and reactions at both side groups and at chains in conjugated molecules.[60,61] For instance, photo-oxidation studies in polyphenylenevinylene derivatives have shown that oxygen incorporation and defect formation leading to reduced conjugation correlate well with alteration of optical properties, such as significantly blue-shifted absorption and reduced emission yield.[60,62,63] To investigate the impact of the CAP treatment on the optical properties of the conjugated polymers, absorption and photoluminescence (PL) measurements are carried out on solutions and fibers, respectively (Figure 5a,b). For both studied molecules, the integrated PL spectra of fibers show variations in the emission peak wavelengths by less than 4% (Table 1), and the solution absorption is almost unaltered following CAP with a peak at 428−430 nm and full width at half-maximum (FWHM), $\Delta\lambda_{Abs}$ = 77−78 nm for PFV, and peak at 457−458 nm and $\Delta\lambda_{Abs}$ = 80−90 nm for F8BT. The blue-shift found for the PL of electrospun PFV fibers upon CAP treatment (Figure 5b) is indicative of relatively reduced energy migration[64] in this class of fibers. Moreover, the measured absolute PL quantum yields (QE) of fibers remain highly stable at 10 and 34% for PFV and F8BT fibers, respectively, regardless of the CAP treatment (Table 1). Overall, the CAP process performed on conjugated

Table 1. Optical Properties of Conjugated Polymer Fibers, Electrospun from either Pristine or CAP-Treated Solutions[a]

parameter	F8BT		PFV	
	CAP-treated	pristine	CAP-treated	pristine
λ_{PL} [nm]	556	555	525	546
$\Delta\lambda_{PL}$ [nm]	78	81	80	90
QE ± ΔQE	0.34 ± 0.04	0.34 ± 0.01	0.10 ± 0.01	0.09 ± 0.02
α [cm^{-1}]	190−380	1200−2000	270−500	760−1500

[a]All the symbols are introduced in the text.

polymer solutions prior to electrospinning appears to offer an excellent combination of improved spinnability and well-preserved optical properties. Indeed, fibers electrospun from CAP-treated solutions of the F8BT and PFV polymers show a bright light emission, uniform along their length as shown in Figure 5c,d. The spectrally resolved confocal micrographs evidence the uniformity of emission from different regions of the conjugated polymer fibers, which can be compared with that from inhomogeneities, including beads spun from pristine solutions (Figure S3), which indicate the onset of different reconfigurational dynamics[65] and possibly local densification phenomena affecting polymer molecules during electrospinning. Figure S4 shows the spatially resolved PL spectra, collected on the different fiber segments highlighted by squares in Figure 5c,d and in Figure S3. The spectra of fibers from CAP-treated solutions show minor differences (∼5%) in their FWHM values (Figure 6a), which may be attributed to the
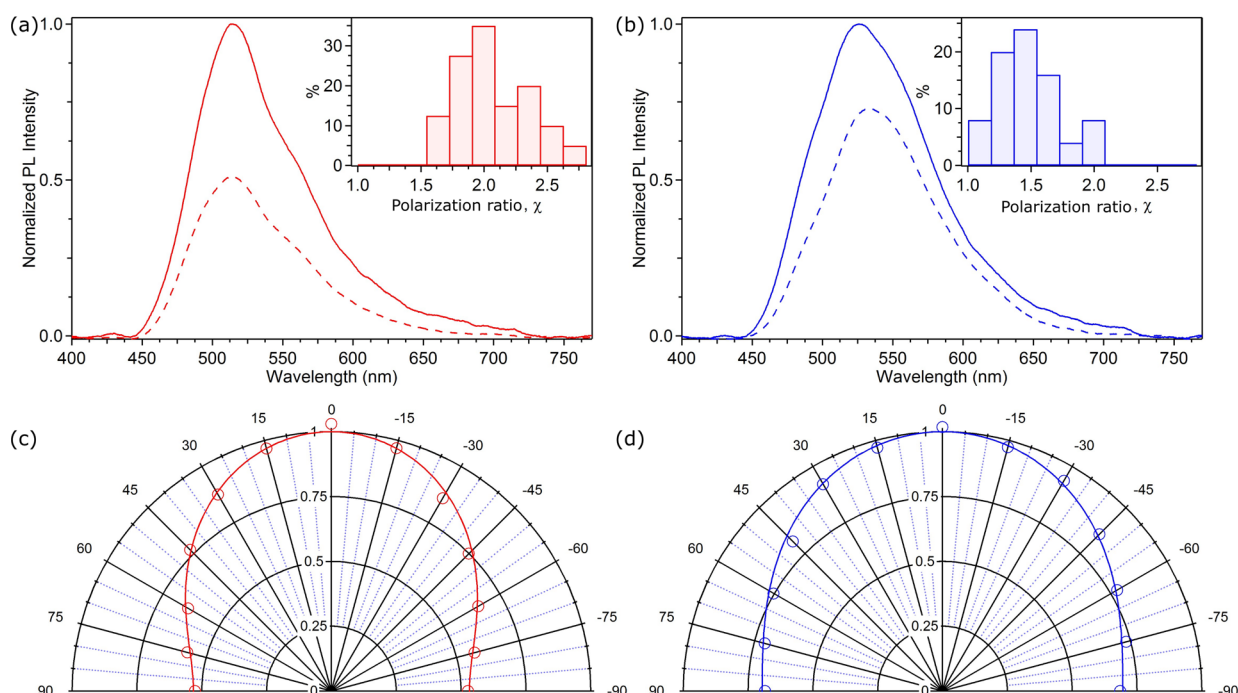
Figure 6. (a,b) PL spectra of individual PFV fibers electrospun from CAP-treated (a) and pristine (b) solutions, measured with the analyzer axis parallel (continuous lines) or perpendicular (dashed lines) to the fiber length. Insets: corresponding distributions of polarization ratio, χ. (c,d) Polar plots of the normalized emission intensity (circles) as a function of the angle of the analyzer polarization filter axis, θ, measured with respect to the fiber longitudinal axis ($\theta = 0°$ for polarizer axis parallel to the fiber length, $\theta = 90°$ for polarizer axis perpendicular to the fiber length). (c) and (d) refer to single fiber spectra from CAP-treated (c) and pristine (d) PFV solutions, respectively. Continuous lines: best fits to data by a $\cos^2(\theta)$ law.

local aggregate formation as favored by the plasma process. Differences up to more than 10% are instead found for widths of spectra of light-emitting fibers spun from pristine solutions.

These aspects relate to the overall order of conjugated polymer macromolecules on a single fiber scale, which can also be probed by polarized micro-photoluminescence (μ-PL). Spectra from individual F8BT and PFV fibers, collected through a polarizer either parallel ($PL_{\parallel}$) or perpendicular ($PL_{\perp}$) to the longitudinal fiber axis, are shown in Figure S5 and in Figure 6, respectively. The statistical distribution of the PL polarization ratio ($\chi = PL_{\parallel}/PL_{\perp}$), estimated on 50 fibers, indicates that, for F8BT and PFV materials spun from pristine solutions, the intensity of $PL_{\parallel}$ is up to 4.5 or up to 2.0 times higher than that of the $PL_{\perp}$ component (insets of Figure S5a,b and Figure 6a,b). The intensity of the PL from individual fibers is also shown as a function of the angle (θ) between the longitudinal axis of the fiber and the emission polarization direction and fitted by the Malus law [$\sim\cos^2(\theta)$] as shown in Figure S5c,d and Figure 6c,d. Interestingly, the alignment of the dipole moments of the transitions from excited states is found to improve upon CAP treatment, supporting the formation of a more ordered phase. Indeed, the maximum χ values increase up to 5.0 and 3.0 for F8BT and PFV fibers, respectively, with a general improvement of polarization in emitted light (see for instance the sharper angular dependence highlighted by the curve in Figure 6c vs Figure 6d).

Even more than the polarized emission, the improved morphology obtained by CAP remarkably affects the self-waveguiding of light emitted by conjugated polymer chromophores along the fiber length. Indeed, the optical losses in light-emitting organic semiconductor waveguides are largely affected by scattering of the guided emission due to

surface roughness and defects associated with an inhomogeneous internal structure. To analyze the propagation losses of light guided by the conjugated polymer fibers, they are deposited on quartz substrates (refractive index 1.46), and the intensity of the PL signal escaping from the fiber body is collected and measured as a function of the distance from the excitation spot, d (Figure 7). Typical PL micrographs of the light-emitting filaments obtained by CAP-treated solutions are shown in Figure 7c,d, showing effective guiding of the photons originating from the focused excitation laser beam. For instance, the light guided along F8BT fibers is clearly appreciable for a distance of up to 0.2 mm from the excitation region (Figure 7c). The measured intensity (I) shows a well-behaved exponential decay upon increasing d, i.e., $I = I_0 \exp(-\alpha d)$, where I_0 is the intensity of the fiber-coupled emission at the excitation region and α indicates the optical loss coefficient. Due to the smoother surface and uniform diameter (Figure 2a,b), much lower optical loss coefficients are obtained for the F8BT fibers electrospun from CAP-treated solutions ($\alpha \cong 190-380$ cm^{-1} vs $\alpha \cong 1200-2000$ cm^{-1} for fibers electrospun from pristine solutions). Similar results are obtained for PFV fibers for which the measured optical loss coefficients decrease from $760-1500$ to $270-500$ cm^{-1} upon CAP treatment of the electrospinning solutions. These values are in line or outperform some of the best ones reported so far for conjugated polymers in nanofibers.[66,67] These results are therefore highly promising in view of developing optical sensors and low-threshold lasers based on active electrospun nanofibers by CAP-treated organic solutions.
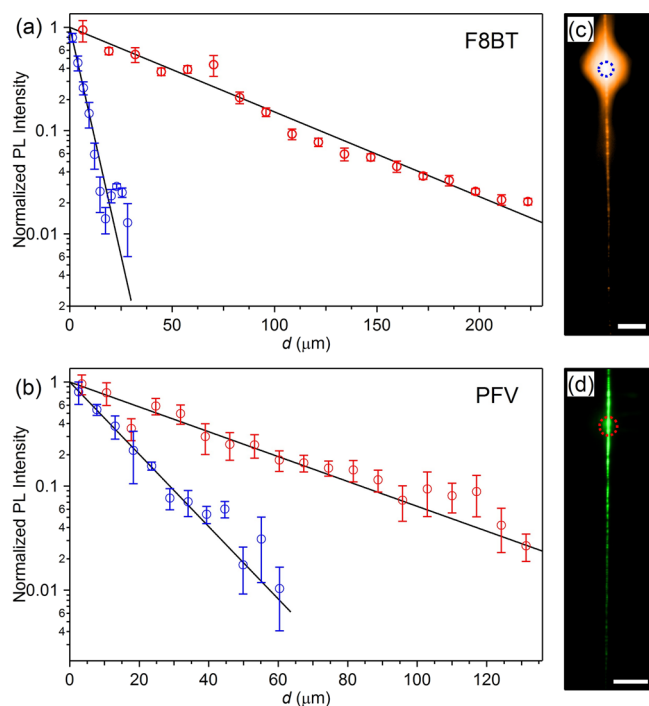
Figure 7. (a,b) Spatial decays of the light intensity guided along individual F8BT (a) and PFV (b) electrospun fibers, as a function of distance, d, from the photoexcitation spot. Red and blue symbols are used for fibers electrospun from CAP-treated and pristine solutions, respectively. The continuous lines are the best fits to experimental data by an exponential function, $I = I_0 \exp(-\alpha d)$ (see the text). (c,d) PL micrographs of single F8BT (c) and PFV (d) fibers made from CAP-treated solutions and excited by a highly focused laser spot. Scale bar = 20 μm.

CONCLUSIONS

Smooth, bead-free light-emitting fibers are realized by electrospinning using for the first time a CAP treatment of solutions of conjugated polymer materials prior to electrospinning. Such a process promotes the production of smoother and more uniform active fibers, with well-preserved optical properties and quantum yield. The polarization of emitted light and especially the optical waveguiding capability are remarkably enhanced compared to fibers produced by standard solutions of conjugated polymers, with an up to 6-fold reduction measured for the optical loss coefficients. These results make the CAP-assisted electrospinning method highly promising for the realization of new organic and hybrid nanomaterials based on conjugated polymers for use in improved light-emitting waveguides for nanophotonics, optical sensors, and organic lasers.

METHODS

Materials and Solution Preparation. F8BT (M_w = 132 kDa) and PFV (M_w = 65 kDa) were purchased from American Dye Source, Inc. THF solutions of the two polymers were prepared at concentrations of 35−70 and 50−100 mg/mL, respectively, and stirred for 12 h at room temperature. Concentrations of solutions for CAP treatment were calibrated to take into account the solvent evaporation occurring during the process.

CAP Treatment. A DBD plasma jet with a 15 cm dielectric tube made from Teflon ($\varnothing_{ext}$ = 4 mm, $\varnothing_{int}$ = 2 mm) was used as the CAP source. As a high-voltage electrode, an Al foil with 30 mm width was wrapped outside the dielectric tube. A 12 cm-long Cu wire (1 mm diameter) and a metallic needle (0.6 mm diameter) were inserted inside and at the end of the tube, respectively, and plasma was generated at the downstream end. Argon was used as a working gas with a flow rate of 100 sccm. The plasma source was driven by a sinusoidal high-voltage pulse generator operating at a peak voltage of 30 kV, frequency of 22 kHz, and duty cycle of 7.5%, with an average power of 6.94 ± 0.08 W. Voltage and current waveforms were collected by a high-voltage probe (Tektronix P6015A) and a current probe (Pearson 6585) connected to an oscilloscope (Tektronix DPO 40034). 1 mL of the polymer solution, which is a reliable volume to perform an electrospinning experiment, was spilled in 1.5 mL tubes (Eppendorf) and CAP-treated immersing the needle of the plasma source by 5 mm below the free surface of the liquid. The suitable duration of the CAP process (5 min) was determined in preliminary experiments to enhance electrospinnability, and the mass of the polymer solution was measured before and after CAP treatment to evaluate the amount of evaporated solvent. The solutions were electrospun or characterized immediately after the CAP treatment.

Electrospinning. Electrospinning experiments were carried out by a 1 mL syringe with a 21 gauge, stainless steel needle, a syringe pump (Harvard Apparatus) for controlled delivery of polymer solutions, a metal collector at a distance of 20−25 cm from the needle tip, and a high-voltage power supply (Glassman Series EH). Briefly, conjugated polymer solutions were transferred into the syringe and injected through to the needle at a constant rate of 0.5 mL/h. A voltage bias of 9−10 kV was applied between the syringe needle and the collector. The distance between the tip of the needle and the collector was fixed at 20 cm for F8BT and 25 cm for PVF fibers. Al foils or quartz slides were employed as fiber deposition targets. Fibers were inspected by SEM at 5 kV. The average diameter and standard deviation values of the fiber diameter distributions were calculated by analyzing ∼300 fibers from the SEM micrographs for each sample.

Calorimetry and Rheology. DSC measurements were carried out using a TA Instruments Q100 system equipped with liquid nitrogen cooling. DSC scans were performed at a heating scan rate of 20 °C/min in a helium atmosphere. Viscosity measurements were carried out with an Anton Paar Rheometer MCR 102 using a cone-plate configuration (50 mm diameter and 1° at the cone tip). Experiments were performed at constant temperature (23 °C) controlled by an integrated Peltier system and a Julabo AWC100 cooling system. A solvent trap (H-PTD200) was used to limit solvent evaporation during measurements. The flow curves of both untreated and plasma-treated solutions of F8BT (70 mg/mL) were acquired at shear rates ranging from 0.3 to 100 s^{-1}.

Light Scattering. Dynamic light scattering from the conjugated polymer solutions was studied by a Malvern Zetasizernano-S working with a 532 nm laser beam. ζ-potential measurements were performed at 25 °C with a dip cell ZEN1002 for organic solutions, used in combination with a glass cell (PCS1115). A 1:500 dilution was used for 70 mg/mL F8BT solutions for reliable ζ-potential measurements.

Spectroscopy. Confocal fluorescence mapping was performed by using a laser scanning microscope (Nikon A1R-MP) equipped with a spectral scan head. The confocal system consisted of an inverted microscope (Eclipse Ti, Nikon), a 20× objective (numerical aperture N.A. = 0.50), and an excitation laser source (λ = 408 nm). The sample emission was collected through the microscope objective, and the intensity was evaluated by the spectral detection scan head fitted out with a multianode photomultiplier. UV−visible absorption spectra of conjugated polymer solutions were collected by using a spectrophotometer (Lambda 950, Perkin Elmer). PL spectra were measured exciting samples by a continuous wave (CW) diode laser (λ = 405 nm, μLS Micro Laser Systems, Inc.) and collecting the emission by a spectrometer (USB 4000, Ocean Optics) through an optical fiber. The absolute quantum efficiency (QE) of the electrospun fibers was estimated by using an integrating sphere (Labsphere), excited by the CW diode laser and measuring PL by a fiber-coupled spectrometer.[68] The spectra were corrected for the spectral response of the apparatus (integrating sphere, optical fiber, and spectrometer). The polarization properties of single active fibers were probed by using a μ-PL system, which is based on an inverted microscope (IX71, Olympus). A laser beam (λ = 405 nm) was focused onto individual

fibers exploiting a dichroic mirror and through the microscope objective (N.A. = 0.5, Olympus, spot diameter of a few microns). A rotating polarized analyzer was used for characterizing the emission polarization state of the individual fibers whose PL was spectrally analyzed by the optical fiber coupled spectrometer. Fiber waveguiding properties were also investigated by the μ-PL system, further equipped with a Peltier-cooled charge-coupled device (Leica, DFC 490). Part of the light emitted by the excited fiber region was coupled into the polymer filament and then waveguided. The optical loss coefficient was estimated analyzing the spatial decay of the light intensity diffused by the fiber surface, as a function of the distance from the exciting laser spot. A polarized optical microscope (Zeiss Axioscope) was used to inspect depositions from CAP-treated and pristine polymer solutions, cast on glass slides and following THF evaporation.

◼ ASSOCIATED CONTENT

Ⓢ Supporting Information

The Supporting Information is available free of charge at https://pubs.acs.org/doi/10.1021/acsami.0c02724.

> Further confocal micrographs, spectroscopic data, and emission polarization data (PDF)

◼ AUTHOR INFORMATION

Corresponding Authors

Maria Letizia Focarete − *Chemistry Department "Giacomo Ciamician" and INSTM UdR of Bologna and Health Sciences and Technologies-Interdepartmental Center for Industrial Research (HST-ICIR), University of Bologna, 40126 Bologna, Italy;* ⓞ orcid.org/0000-0002-0458-7836; Email: marialetizia.focarete@unibo.it

Dario Pisignano − *NEST, Istituto Nanoscienze-CNR and Scuola Normale Superiore, I-56127 Pisa, Italy; Dipartimento di Fisica, Università di Pisa, I-56127 Pisa, Italy;* ⓞ orcid.org/0000-0003-3758-5199; Email: dario.pisignano@unipi.it

Authors

Vito Fasano − *Dipartimento di Matematica e Fisica "Ennio De Giorgi", Università del Salento, I-73100 Lecce, Italy;* ⓞ orcid.org/0000-0001-9607-9726

Romolo Laurita − *Department of Industrial Engineering (DIN), Università di Bologna, 40123 Bologna, Italy; Advanced Mechanics and Materials-Interdepartmental Center, University of Bologna, 40123 Bologna, Italy*

Maria Moffa − *NEST, Istituto Nanoscienze-CNR and Scuola Normale Superiore, I-56127 Pisa, Italy*

Chiara Gualandi − *Advanced Mechanics and Materials-Interdepartmental Center and Chemistry Department "Giacomo Ciamician" and INSTM UdR of Bologna, University of Bologna, 40123 Bologna, Italy;* ⓞ orcid.org/0000-0002-2020-1892

Vittorio Colombo − *Department of Industrial Engineering (DIN), Università di Bologna, 40123 Bologna, Italy; Advanced Mechanics and Materials-Interdepartmental Center, University of Bologna, 40123 Bologna, Italy*

Matteo Gherardi − *Department of Industrial Engineering (DIN), Università di Bologna, 40123 Bologna, Italy; Advanced Mechanics and Materials-Interdepartmental Center, University of Bologna, 40123 Bologna, Italy*

Eyal Zussman − *Department of Mechanical Engineering, Technion − Israel Institute of Technology, Haifa 32000, Israel*

Gleb Vasilyev − *Department of Mechanical Engineering, Technion − Israel Institute of Technology, Haifa 32000, Israel*

Luana Persano − *NEST, Istituto Nanoscienze-CNR and Scuola Normale Superiore, I-56127 Pisa, Italy*

Andrea Camposeo − *NEST, Istituto Nanoscienze-CNR and Scuola Normale Superiore, I-56127 Pisa, Italy*

Complete contact information is available at:
https://pubs.acs.org/10.1021/acsami.0c02724

Author Contributions

[+]V.F. and R.L. equally contributed to this paper. The manuscript was written through contributions of all authors. All authors have given approval to the final version of the manuscript.

Notes

The authors declare no competing financial interest.

◼ ACKNOWLEDGMENTS

◼ REFERENCES

(1) O'Carroll, D.; Lieberwirth, I.; Redmond, G. Microcavity Effects and Optically Pumped Lasing in Single Conjugated Polymer Nanowires. *Nat. Nanotechnol.* **2007**, *2*, 180−184.

(2) Vohra, V.; Giovanella, U.; Tubino, R.; Murata, H.; Botta, C. Electroluminescence from Conjugated Polymer Electrospun Nanofibers in Solution Processable Organic Light-Emitting Diodes. *ACS Nano* **2011**, *5*, 5572−5578.

(3) Persano, L.; Camposeo, A.; Del Carro, P.; Fasano, V.; Moffa, M.; Manco, R.; D'Agostino, S.; Pisignano, D. Distributed Feedback Imprinted Electrospun Fiber Lasers. *Adv. Mater.* **2014**, *26*, 6542−6547.

(4) Gaio, M.; Saxena, D.; Bertolotti, J.; Pisignano, D.; Camposeo, A.; Sapienza, R. A Nanophotonic Laser on a Graph. *Nat. Commun.* **2019**, *10*, 226.

(5) Lee, S. W.; Lee, H. J.; Choi, J. H.; Koh, W. G.; Myoung, J. M.; Hur, J. H.; Park, J. J.; Cho, J. H.; Jeong, U. Periodic Array of Polyelectrolyte-Gated Organic Transistors from Electrospun Poly (3-hexylthiophene) Nanofibers. *Nano Lett.* **2010**, *10*, 347−351.

(6) Kim, F. S.; Ren, G.; Jenekhe, S. A. One-Dimensional Nanostructures of π-Conjugated Molecular Systems: Assembly, Properties, and Applications from Photovoltaics, Sensors, and Nanophotonics to Nanoelectronics. *Chem. Mater.* **2011**, *23*, 682−732.

(7) Wang, S.; Kappl, M.; Liebewirth, I.; Müller, M.; Kirchhoff, K.; Pisula, W.; Müllen, K. Organic Field-Effect Transistors Based on Highly Ordered Single Polymer Fibers. *Adv. Mater.* **2012**, *24*, 417−420.

(8) Kweon, O. Y.; Lee, S. J.; Oh, J. H. Wearable High-Performance Pressure Sensors Based on Three-Dimensional Electrospun Conductive Nanofibers. *NPG Asia Mater.* **2018**, *10*, 540−551.

(9) Chang, C.; Tran, V. H.; Wang, J.; Fuh, Y.-K.; Lin, L. Direct-Write Piezoelectric Polymeric Nanogenerator with High Energy Conversion Efficiency. *Nano Lett.* **2010**, *10*, 726−731.

(10) Qin, Z.; Chen, X.; Yin, Y.; Ma, G.; Jia, Y.; Deng, J.; Pan, K. Flexible Janus Electrospun Nanofiber Films for Wearable Triboelectric Nanogenerator. *Adv. Mater. Technol.* **2019**, *5*, 1900859.

(11) Asai, H.; Okumura, T.; Sakamoto, H.; Nakane, K. Effect of Polymer Type on the Performance of a Nanofiber Mat Actuator. *Polym. J.* **2019**, *51*, 523−528.

(12) Ma, Z.; Hu, Z.; Zhang, H.; Peng, M.; He, X.; Li, Y.; Yang, Z.; Qiu, J. Flexible and Transparent Optically Anisotropic Films Based on Oriented Assembly of Nanofibers. *J. Mater. Chem. C* **2016**, *4*, 1029−1038.

(13) Arinstein, A.; Burman, M.; Gendelman, O.; Zussman, E. Effect of Supramolecular Structure on Polymer Nanofibre Elasticity. *Nat. Nanotechnol.* **2007**, *2*, 59−62.

(14) Xia, H.; Wang, R.; Liu, Y.; Cheng, J.; Zou, G.; Zhang, Q.; Zhang, D.; Wang, P.; Ming, H.; Badugu, R.; Lakowicz, J. R. Active Polymer Microfiber with Controlled Polarization Sensitivity. *Adv. Opt. Mater.* **2016**, *4*, 371−377.

(15) Shen, S.; Henry, A.; Tong, J.; Zheng, R.; Chen, G. Polyethylene Nanofibres with Very High Thermal Conductivities. *Nat. Nanotechnol.* **2010**, *5*, 251−255.

(16) Xia, Y.; Yang, P.; Sun, Y.; Wu, Y.; Mayers, B.; Gates, B.; Yin, Y.; Kim, F.; Yan, H. One-dimensional Nanostructures: Synthesis, Characterization, and Applications. *Adv. Mater.* **2003**, *15*, 353−389.

(17) Pisignano, D. *Polymer Nanofibers: Building Blocks for Nanotechnology*; Royal Society of Chemistry: Cambridge, 2013.

(18) Persano, L.; Camposeo, A.; Pisignano, D. Integrated Bottom-up and Top-down Soft Lithographies and Microfabrication Approaches to Multifunctional Polymers. *J. Mater. Chem. C* **2013**, *1*, 7663−7680.

(19) Huang, J.; Virji, S.; Weiller, B. H.; Kaner, R. B. Polyaniline Nanofibers: Facile Synthesis and Chemical Sensors. *J. Am. Chem. Soc.* **2003**, *125*, 314−315.

(20) Martin, C. R. Membrane-based Synthesis of Nanomaterials. *Chem. Mater.* **1996**, *8*, 1739−1746.

(21) Liu, J.; Sheina, E.; Kowalewski, T.; McCullough, R. D. Tuning the Electrical Conductivity and Self-Assembly of Regioregular Polythiophene by Block Copolymerization: Nanowire Morphologies in New Di- and Triblock Copolymers. *Angew. Chem. Int. Ed.* **2002**, *41*, 329−332.

(22) Samitsu, S.; Shimomura, T.; Heike, S.; Hashizume, T.; Ito, K. Field-Effect Carrier Transport in Poly(3-alkylthiophene) Nanofiber Networks and Isolated Nanofibers. *Macromolecules* **2010**, *43*, 7891−7894.

(23) Sinha-Ray, S.; Sinha-Ray, S.; Yarin, A. L.; Pourdeyhimi, B. Theoretical and Experimental Investigation of Physical Mechanisms Responsible for Polymer Nanofiber Formation in Solution Blowing. *Polymer* **2015**, *56*, 452−463.

(24) Reneker, D. H.; Chun, I. Nanometre Diameter Fibres of Polymer, Produced by Electrospinning. *Nanotechnology* **1996**, *7*, 216−223.

(25) Greiner, A.; Wendorff, J. H. Electrospinning: a Fascinating Method for the Preparation of Ultrathin Fibers. *Angew. Chem. Int. Ed.* **2007**, *46*, 5670−5703.

(26) Li, D.; Xia, Y. Electrospinning of Nanofibers: Reinventing the Wheel? *Adv. Mater.* **2004**, *16*, 1151−1170.

(27) Teo, W. E.; Ramakrishna, S. A Review on Electrospinning Design and Nanofibre Assemblies. *Nanotechnology* **2006**, *17*, R89−R106.

(28) Li, D.; Wang, Y.; Xia, Y. Electrospinning of Polymeric and Ceramic Nanofibers as Uniaxially Aligned Arrays. *Nano Lett.* **2003**, *3*, 1167−1171.

(29) Sun, D.; Chang, C.; Li, S.; Lin, L. Near-Field Electrospinning. *Nano Lett.* **2006**, *6*, 839−842.

(30) Di Camillo, D.; Fasano, V.; Ruggieri, F.; Santucci, S.; Lozzi, L.; Camposeo, A.; Pisignano, D. Near-Field Electrospinning of Light-Emitting Conjugated Polymer Nanofibers. *Nanoscale* **2013**, *5*, 11637−11642.

(31) Pagliara, S.; Vitiello, M. S.; Camposeo, A.; Polini, A.; Cingolani, R.; Scamarcio, G.; Pisignano, D. Optical Anisotropy in Single Light-Emitting Polymer Nanofibers. *J. Phys. Chem. C* **2011**, *115*, 20399−20405.

(32) Kakade, M. V.; Givens, S.; Gardner, K.; Lee, K. H.; Chase, D. B.; Rabolt, J. F. Electric Field Induced Orientation of Polymer Chains in Macroscopically Aligned Electrospun Polymer Nanofibers. *J. Am. Chem. Soc.* **2007**, *129*, 2777−2782.

(33) Gazzano, M.; Gualandi, C.; Zucchelli, A.; Sui, T.; Korsunsky, A. M.; Reinhard, C.; Focarete, M. L. Structure-Morphology Correlation in Electrospun Fibers of Semicrystalline Polymers by Simultaneous Synchrotron SAXS-WAXD. *Polymer* **2015**, *63*, 154−163.

(34) MacDiarmid, A. G. Synthetic Metals: a Novel Role for Organic Polymers (Nobel Lecture). *Angew. Chem. Int. Ed.* **2001**, *40*, 2581−2590.

(35) Heeger, A. J. Semiconducting and Metallic Polymers: the Fourth Generation of Polymeric Materials (Nobel Lecture). *Angew. Chem. Int. Ed.* **2001**, *40*, 2591−2611.

(36) Facchetti, A. π-Conjugated Polymers for Organic Electronics and Photovoltaic Cell Applications. *Chem. Mater.* **2011**, *23*, 733−758.

(37) Li, D.; Babel, A.; Jenekhe, S. A.; Xia, Y. Nanofibers of Conjugated Polymers Prepared by Electrospinning with a Two-Capillary Spinneret. *Adv. Mater.* **2004**, *16*, 2062−2066.

(38) Babel, A.; Li, D.; Xia, Y.; Jenekhe, S. A. Electrospun Nanofibers of Blends of Conjugated Polymers: Morphology, Optical Properties, and Field-Effect Transistors. *Macromolecules* **2005**, *38*, 4705−4711.

(39) Di Benedetto, F.; Camposeo, A.; Pagliara, S.; Mele, E.; Persano, L.; Stabile, R.; Cingolani, R.; Pisignano, D. Patterning of Light-Emitting Conjugated Polymer Nanofibres. *Nat. Nanotechnol.* **2008**, *3*, 614−619.

(40) Bounioux, C.; Avrahami, R.; Vasilyev, G.; Patil, N.; Zussman, E.; Yerushalmi-Rozen, R. Single-step Electrospinning of Multi Walled Carbon Nanotubes−Poly(3-octylthiophene) Hybrid Nano-Fibers. *Polymer* **2016**, *86*, 15−21.

(41) Campoy-Quiles, M.; Ishii, Y.; Sakai, H.; Murata, H. Highly Polarized Luminescence from Aligned Conjugated Polymer Electrospun Nanofibers. *Appl. Phys. Lett.* **2008**, *92*, 213305.

(42) Zhou, R.; Chen, W.; Jiang, X.; Wang, S.; Gong, Q. Enhanced Exciton Migration in Electrospun Poly[2-methoxy-5-(2′-ethylhexyloxy)-1, 4-phenylenevinylene]/poly (vinyl pyrrolidone) Nanofibers. *Appl. Phys. Lett.* **2010**, *96*, 133309.

(43) Kim, M.; Jo, S. B.; Park, J. H.; Cho, K. Flexible Lateral Organic Solar Cells With Core−Shell Structured Organic Nanofibers. *Nano Energy* **2015**, *18*, 97−108.

(44) Okuzaki, H.; Takahashi, T.; Miyajima, N.; Suzuki, Y.; Kuwabara, T. Spontaneous Formation of Poly(*p*-phenylenevinylene) Nanofiber Yarns through Electrospinning of a Precursor. *Macromolecules* **2006**, *39*, 4276−4278.

(45) Xin, Y.; Huang, Z.; Jiang, Z.; Li, D.; Peng, L.; Zhai, J.; Wang, D. Photoresponse of a Single Poly(*p*-phenylene vinylene)-CdSe Bulk-Heterojunction Submicron Fiber. *Chem. Commun.* **2010**, *46*, 2316−2318.

(46) Zhong, W.; Li, F.; Chen, L.; Chen, Y.; Wei, Y. A Novel Approach to Electrospinning of Pristine and Aligned MEH-PPV Using Binary Solvents. *J. Mater. Chem.* **2012**, *22*, 5523−5530.

(47) Madhugiri, S.; Dalton, A.; Gutierrez, J.; Ferraris, J. P.; Balkus, K. J. Electrospun MEH-PPV/SBA-15 Composite Nanofibers Using a Dual Syringe Method. *J. Am. Chem. Soc.* **2003**, *125*, 14531−14538.

(48) Shi, Q.; Vitchuli, N.; Nowak, J.; Lin, Z.; Guo, B.; Mccord, M.; Bourham, M.; Zhang, X. Atmospheric Plasma Treatment of Pre-electrospinning Polymer Solution: A Feasible Method to Improve Electrospinnability. *J. Polym. Sci., Part B: Polym. Phys.* **2011**, *49*, 115−122.

(49) Rezaei, F.; Vanraes, P.; Nikiforov, A.; Morent, R.; De Geyter, N. Applications of Plasma-Liquid Systems: A Review. *Materials* **2019**, *12*, 2751.

(50) Colombo, V.; Fabiani, D.; Focarete, M. L.; Gherardi, M.; Gualandi, C.; Laurita, R.; Zaccaria, M. Atmospheric Pressure Non-equilibrium Plasma Treatment to Improve the Electrospinnability of Poly(L-lactic acid) Polymeric Solution. *Plasma Process. Polym.* **2014**, *11*, 247−255.

(51) Laurita, R.; Zaccaria, M.; Gherardi, M.; Fabiani, D.; Merlettini, A.; Pollicino, A.; Focarete, M. L.; Colombo, V. Plasma Processing of Electrospun Li-Ion Battery Separators to Improve Electrolyte Uptake. *Plasma Processes Polym.* **2016**, *13*, 124−133.

(52) Grande, S.; Van Guyse, J.; Nikiforov, A. Y.; Onyshchenko, I.; Asadian, M.; Morent, R.; Hoogenboom, R.; De Geyter, N. Atmospheric Pressure Plasma Jet Treatment of Poly-ε-caprolactone Polymer Solutions to Improve Electrospinning. *ACS Appl. Mater. Interfaces* **2017**, *9*, 33080−33090.

(53) Bruggeman, P.; Leys, C. Non-Thermal Plasmas in and in Contact with Liquids. *J. Phys. D: Appl. Phys.* **2009**, *42*, No. 053001.

(54) Lu, Y.; Xu, S. F.; Zhong, X. X.; Ostrikov, K.; Cvelbar, U.; Mariotti, D. Characterization of a DC-Driven Microplasma Between a Capillary Tube and Water Surface. *Europhys. Lett.* **2013**, *102*, 15002.

(55) Banach, M. J.; Friend, R. H.; Sirringhaus, H. Influence of the Molecular Weight on the Thermotropic Alignment of Thin Liquid Crystalline Polyfluorene Copolymer Films. *Macromolecules* **2003**, *36*, 2838−2844.

(56) Chen, J.-W.; Huang, C.-C.; Chao, C. Y. Supramolecular Liquid-Crystal Gels Formed by Polyfluorene-Based π-Conjugated Polymer for Switchable Anisotropic Scattering Device. *ACS Appl. Mater. Interfaces* **2014**, *6*, 6757−6764.

(57) Choe, E. W.; Kim, S. N. Synthesis, Spinning, and Fiber Mechanical Properties of Poly (p-phenylenebenzobisoxazole). *Macromolecules* **1981**, *14*, 920−924.

(58) Onogi, S.; Asada, T. Rheology and Rheo-Optics of Polymer Liquid Crystals. In *Rheology*; Astarita, G., Marrucci, G., Nicolais, L., Eds.; Plenum Press: New York, 1980, 122.

(59) Zaumseil, J.; Kline, R. J.; Sirringhaus, H. Electroluminescence Imaging and Microstructure of Organic Light-Emitting Field-Effect Transistors. *Appl. Phys. Lett.* **2008**, *92*, No. 073304.

(60) Yan, M.; Rothberg, L. J.; Papadimitrakopoulos, F.; Galvin, M. E.; Miller, T. M. Defect Quenching of Conjugated Polymer Luminescence. *Phys. Rev. Lett.* **1994**, *73*, 744−747.

(61) Brabec, C.; Egelhaaf, H. J.; Salvador, M. The Path to Ubiquitous Organic Electronics Hinges on its Stability. *J. Mater. Res.* **2018**, *33*, 1839−1840.

(62) Rothberg, L. J.; Yan, M.; Papadimitrakopoulos, F.; Galvin, M. E.; Kwock, E. W.; Miller, T. M. Photophysics of Phenylenevinylene Polymers. *Synth. Met.* **1996**, *80*, 41−58.

(63) Golovnin, I. V.; Bakulin, A. A.; Zapunidy, S. A.; Nechvolodova, E. M.; Paraschuk, D. Y. Dramatic Enhancement of Photo-Oxidation Stability of a Conjugated Polymer in Blends with Organic Acceptor. *Appl. Phys. Lett.* **2008**, *92*, 243311.

(64) Hwang, I.; Scholes, G. D. Electronic Energy Transfer and Quantum-Coherence in π-Conjugated Polymers. *Chem. Mater.* **2011**, *23*, 610−620.

(65) Camposeo, A.; Greenfeld, I.; Tantussi, F.; Moffa, M.; Fuso, F.; Allegrini, M.; Zussman, E.; Pisignano, D. Conformational Evolution of Elongated Polymer Solutions Tailors the Polarization of Light-Emission from Organic Nanofibers. *Macromolecules* **2014**, *47*, 4704−4710.

(66) O'Carroll, D.; Lieberwirth, I.; Redmond, G. Melt-Processed Polyfluorene Nanowires as Active Waveguides. *Small* **2007**, *3*, 1178−1183.

(67) Fasano, V.; Polini, A.; Morello, G.; Moffa, M.; Camposeo, A.; Pisignano, D. Bright Light Emission and Waveguiding in Conjugated Polymer Nanofibers Electrospun from Organic Salt Added Solutions. *Macromolecules* **2013**, *46*, 5935−5942.

(68) Greenham, N. C.; Samuel, I. D. W.; Hayes, G. R.; Phillips, R. T.; Kessener, Y. A. R. R.; Moratti, S. C.; Holmes, A. B.; Friend, R. H. Measurement of Absolute Photoluminescence Quantum Efficiencies in Conjugated Polymers. *Chem. Phys. Lett.* **1995**, *241*, 89−96.

Supporting Information

Enhanced electrospinning of active organic fibers by plasma treatment on conjugated polymer solutions

Vito Fasano,[†,+] Romolo Laurita,[§,#,+] Maria Moffa,[‡] Chiara Gualandi,[#,⊥] Vittorio Colombo,[§,#] Matteo Gherardi,[§,#] Eyal Zussman,[∇] Gleb Vasilyev,[∇] Luana Persano,[‡] Andrea Camposeo,[‡] Maria Letizia Focarete,[,⊥,‖] and Dario Pisignano[*,‡,¶]*

[†] Dipartimento di Matematica e Fisica "Ennio De Giorgi", Università del Salento, via Arnesano, I-73100, Lecce, Italy

[§] Department of Industrial Engineering (DIN), Università di Bologna, Viale del Risorgimento 2, 40123 Bologna, Italy

[#] Advanced Mechanics and Materials-Interdepartmental Center, University of Bologna, Viale del Risorgimento 2, 40123 Bologna, Italy

[‡] NEST, Istituto Nanoscienze-CNR and Scuola Normale Superiore, Piazza S. Silvestro 12, I-56127 Pisa, Italy

[⊥] Chemistry Department "Giacomo Ciamician" and INSTM UdR of Bologna, University of Bologna, via Selmi 2, 40126, Bologna, Italy. *E-mail: marialetizia.focarete@unibo.it

[∇] Department of Mechanical Engineering, Technion – Israel Institute of Technology, Haifa 32000, Israel

[‖] Health Sciences and Technologies-Interdepartmental Center for Industrial Research (HST-ICIR), University of Bologna, Via Tolara di Sopra 41/E, Ozzano Emilia I-40064, Italy

[¶] Dipartimento di Fisica, Università di Pisa, Largo B. Pontecorvo 3, I-56127 Pisa, Italy. **E-mail: dario.pisignano@unipi.it
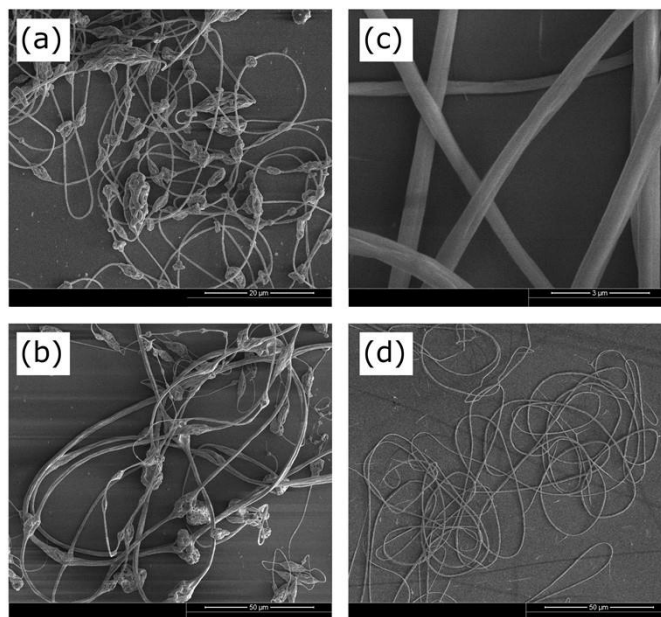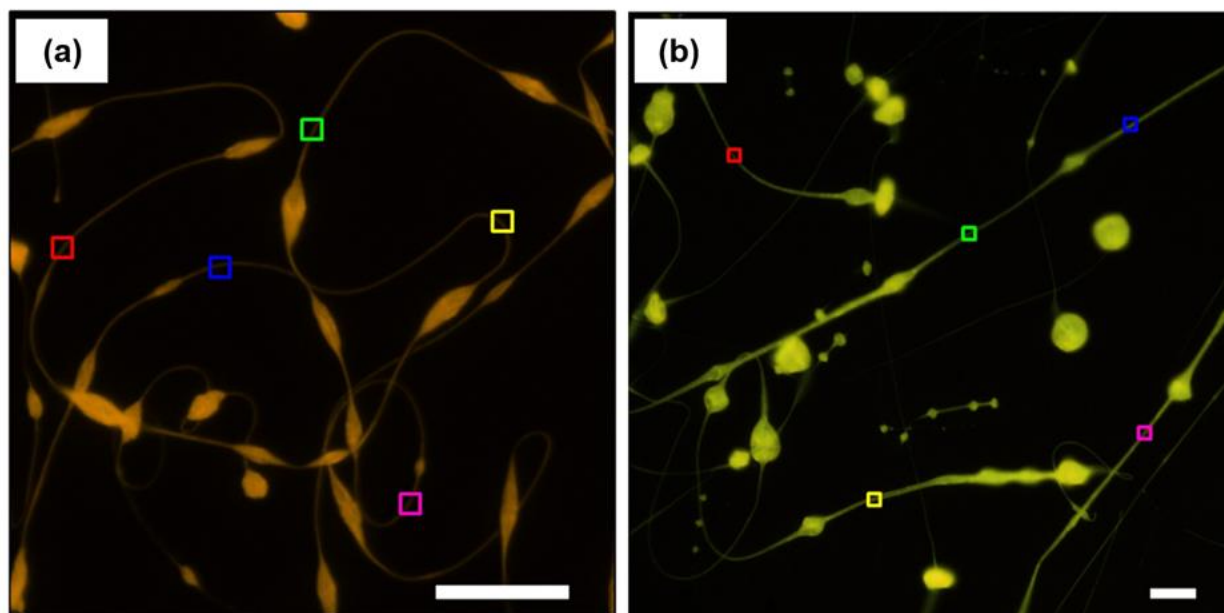
Figure S1. SEM micrographs, collected at different magnifications, of F8BT fibers, electrospun from pristine (a,b) and CAP-treated (c,d) solutions.
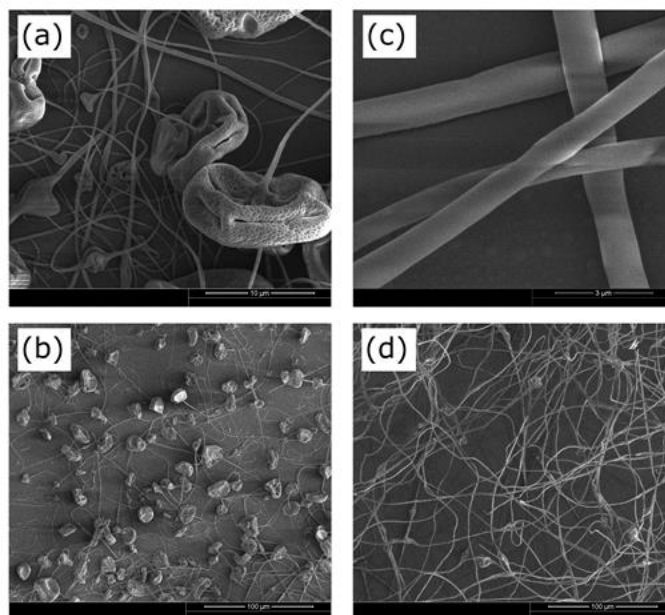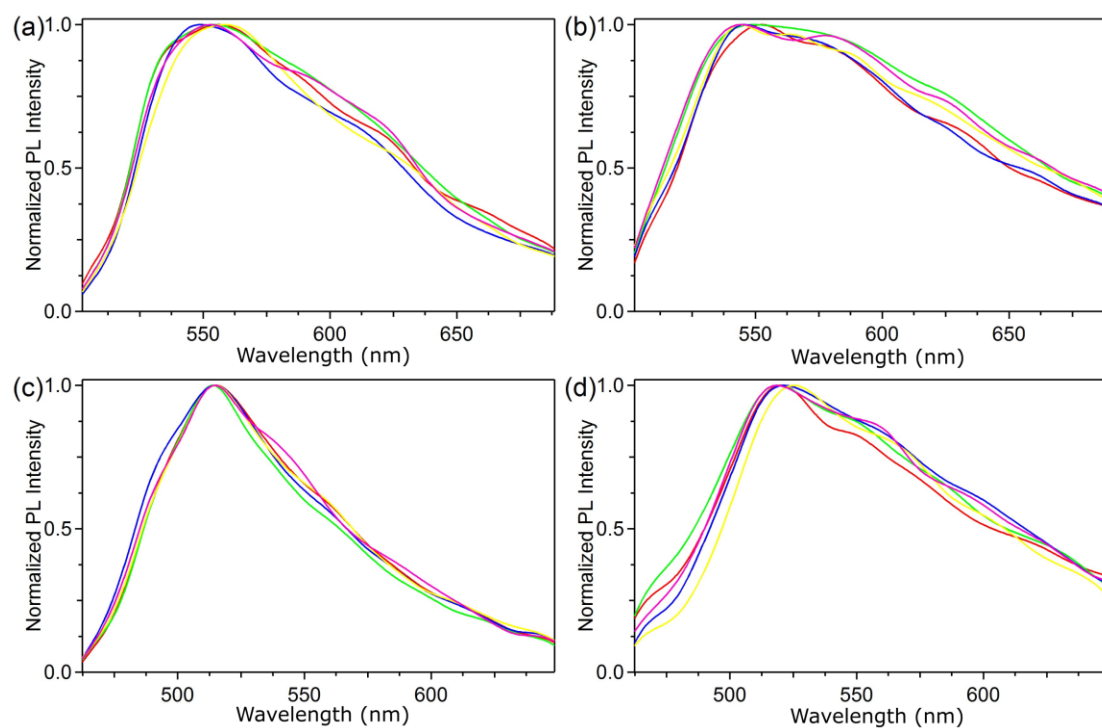

Figure S2. SEM micrographs, collected at different magnifications, of PFV fibers, electrospun from pristine (a,b) and CAP-treated (c,d) solutions.

Figure S3. Fluorescence confocal micrographs of light-emitting fibers electrospun from pristine F8BT (c) and PFV (d) solutions. Excitation wavelength 408 nm. Scale bar = 20 µm.

Figure S4. Spatially-resolved PL spectra of light-emitting fibers electrospun from either CAP-treated (a, c) or pristine (b, d) solutions of F8BT (a, b) and PFV (c, d). Each spectrum is collected in a different region of fibers (squares in the Fig. 5 of the main paper and in Fig. S3), and normalized to its maximum.
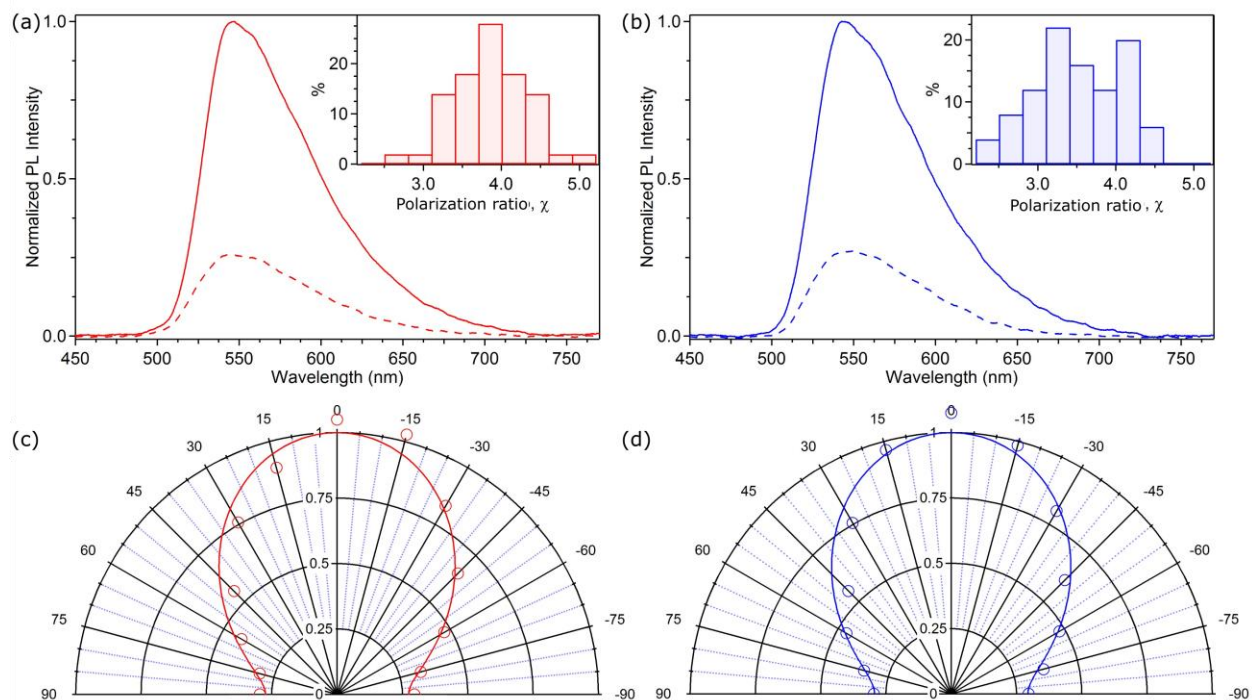
Figure S5. (a,b) PL spectra of individual F8BT fibers electrospun from CAP-treated (a) and pristine (b) solutions, measured with the analyzer axis parallel (continuous lines) or perpendicular (dashed lines) to the fiber length. Insets: corresponding distributions of polarization ratio, χ. (c,d) Polar plots of the normalized emission intensity (circles) as a function of the angle of the analyzer polarization filter axis, θ, measured with respect to the fiber longitudinal axis ($\theta = 0°$ for polarizer axis parallel to the fiber length, $\theta = 90°$ for polarizer axis perpendicular to the fiber length). (c) and (d) refer to single fiber spectra from CAP-treated (c) and pristine (d) F8BT solutions, respectively. Continuous lines: best fits to data by a $\cos^2(\theta)$ law.